

Enhancement of Cloud-Associated Shadow Areas in Satellite Images Using Wavelet Image Fusion

¹A. Abd-Elrahman, ²I.F. Shaker, ³A.K. Abdel-Gawad and ³A. Abdel-Wahab

¹School of Forest Resources and Conservation, Geomatics, University of Florida,

²Public Works Department, Ain Shams University, Cairo, Egypt

³Department of Civil Eng., Engineering Research Division, National Research Center, Cairo, Egypt

Abstract: Shadows created by small patches of clouds obscure ground features from satellite imagery. In this research, a new technique was developed to enhance cloud-associated shadow areas in satellite images while preserving details underneath these areas. The developed algorithm utilizes wavelet analysis to decompose cloudy images into several frequency level components. Image details underneath shadow areas are preserved in the output image by fusing the cloudy image with another cloud-free image. The developed technique is implemented on a cloudy Landsat7 Panchromatic subscene. The results showed that the developed technique was successful in enhancing the cloudy image through preserving the obscured details underneath the cloud-associated shadow. The ability to maintain such details under shadow areas and the amount of introduced artifacts increased with the increase of the wavelet decomposition level. Generally, two or three wavelet decomposition levels were found to be sufficient for the analysis used in this study. The results obtained when using two images with the same spatial resolution were found to be better than those obtained using images with different spatial resolution.

Key words: Wavelet • Fusion • Shadow • Frequency decomposition • Landsat

INTRODUCTION

Space satellite imagery is very cost effective in mapping extended regions. This imagery is historically utilized in mapping roads, hydrological features, vegetation, etc. The existence of high quality images enabled mapping changes in land development in the last two decades. Nevertheless, one of the problems that hindered the use of such imagery is the existence of clouds and their associated shadows. Although cloud areas can easily be detected and replaced from other imagery due to their high reflectance, the shadows caused by these clouds represent areas with low illumination conditions that double the image defected areas. This effect of clouds and cloud-associated shadows are widely spread with approximately 66% of the earth surface is covered by clouds throughout the year [1].

Several methods were used to restore the image content in shadow areas. Some of these methods identifies and removes the image illumination variations using surface reflectance and variations constraints [2, 3]. Such methods were implemented mostly on high spatial

resolution imagery and suffer costly computational overhead in addition to shadow edge processing problems. Other methods utilized overlapping imagery to detect occlusion and remove shadows [4]. Fusion techniques were also used to account for cloud and shadow defects on certain image using different cloud/shadow free images [5, 6]. Although these methods are widely used, they tend to ignore the spatial content underneath shadow areas. Hence, this research is devoted to developing a technique to reduce the effect of cloud-associated shadows using image wavelet decomposition techniques. Although this research deals with a specific type of shadow, the developed technique could be extended to handle other types of shadows resulting from, for example, high buildings and trees.

A milestone in developing such a technique is to be able to automatically detect clouds and shadows in the images. Features utilized for cloud and shadow detection can be classified into three domains [7]: spectral, spatial and temporal. Spectral features, such as image gray levels or color information, are commonly used. Some approaches improve results by using spatial

information working on a regional level, instead of pixel level. Some other methods utilize temporal redundancy to integrate and improve results.

Many algorithms are available to detect clouds and their associated shadows. Concepts such as simple thresholding, neural networks, fuzzy logic, etc were utilized in these algorithms [8]. Scene properties such as scene date and time, sensor and sun locations, etc, although not used in this implementation, could also be utilized in the cloud and shadow detection process. The methodology applied in this research utilizes cloud/shadow geometric constraints in addition to their spectral characteristics [9].

One of the objectives of the methodology developed in this research is to enhance shadow areas by preserving details underneath these shadows. A wavelet decomposition technique is suggested to achieve this objective by fusing this image with another cloud-free image. The results of this technique depend on the accuracy of the cloud/shadow detection process and on the fusion algorithm.

It should be mentioned here that this research is only concerned with shadow areas. Unlike shadow areas, cloud regions are generally opaque and do not have image details underneath. Accordingly, the techniques developed in this study, which utilizes wavelet image fusion to capture details information, was applied only in shadow areas. On the other hand, to enhance the overall output image, clouds were substituted for directly using traditional pixel to pixel replacement from another cloud-free image.

BACKGROUND

In this section background information related to wavelet image decomposition and image fusion is reviewed.

Discrete Wavelet Transform: Wavelet decomposition and reconstruction was historically used in image fusion and image compression applications. Discrete wavelet transform will be utilized in this research to enhance cloud-related shadow areas by adjusting their frequency content. For discrete wavelet transform, let $\phi_{jk} = \phi(2^j x - k)$ and $\psi_{jk} = \psi(2^j x - k)$ be sets of dilated and scaled mother and wavelet functions, respectively. Both functions can be constructed from the higher level scaling functions [10]:

$$\phi(2^{j-1} x) = \sum_k h_{j+1}(k) \phi(2^j x - k) \quad (1)$$

$$\psi(2^{j-1} x) = \sum_k g_{j+1}(k) \phi(2^j x - k) \quad (2)$$

Where $h(k)$ and $g(k)$ are low and high pass filters respectively. Any function $f(x)$ can be represented by given scaling function and its wavelet derivatives as:

$$f(x) = \sum_k c_{j-1_0}(k) \phi(2^{j-1} x - k) + \sum_k d_{j-1}(k) \psi_{j,k}(2^{j-1} x - k) \quad (3)$$

For orthonormal scaling and wavelet functions the scaling (approximation) and wavelet (detail) coefficients can be represented in terms of their values in a previous scale as follows:

$$c_{j-1}(k) = \sum_m h(m - 2k) c_j(m) \quad (4)$$

$$d_{j-1}(k) = \sum_m g(m - 2k) d_j(m) \quad (5)$$

Recalling that the scaling filter is a low pass filter and the wavelet filter is a high pass filter, it can be concluded that obtaining the approximation and detail coefficient constitutes a single step in a an iterative filter bank that results in multiple level decomposition of the signal. This iterative filter bank forms the basis of the discrete wavelet transform. A reverse operation can also be used to completely reconstruct the signal. In image analysis, a generalized form of the one-dimensional discrete wavelet transform can be used. This means that four components are obtained at each wavelet decomposition level. These components are calculated through filtering the image using high and low pass filters.

For an image $f(x, y)$ of size $M \times N$, at each decomposition level, the results are one smooth image resulting from the filtering of the input image using low pass filters in the horizontal and vertical directions. The resulting component is denoted $f_{LL}(x, y)$ and called approximation subimage. Three other details subimages $f_{LH}(x, y)$, $f_{HL}(x, y)$ and $f_{HH}(x, y)$ result from filtering the original images by a combination of low and high pass filters in the horizontal and vertical directions. These three subimages represent decomposition details in the horizontal, vertical and diagonal directions, respectively. It should be mentioned here that the size of the obtained subimages at each decomposition level is half the size of the original image. The approximation subimage could, in turn, be composed to produce the next image decomposition level.

Image Fusion: Generally, image fusion can be defined as the combination of two or more images to form a new

image using certain algorithms [11]. Fusing two images in order to get rid of defective parts in one of the images is a typical image fusion application. Image fusion is performed at three different processing levels according to the stage at which the fusion takes place [12]. These three processing levels are pixel, feature and decision levels. Image fusion at pixel level means fusion at the lowest processing level, referring to the merging of measured physical parameters. Most research utilizing image fusion techniques to correct for image defects tackle pixel-based image fusion, which presumes accurately registered imagery [13].

Fusion at the feature level requires the extraction of objects recognized in the various data sources, e.g., using segmentation procedures. Features correspond to characteristics extracted from the initial images, which depend on the feature's environment such as extent, shape and neighborhood [14]. Decision level fusion is a method that uses interpreted data where the input images are processed individually for information extraction. The obtained information is then combined by applying decision rules to reinforce common interpretation, resolve differences and furnish a better understanding of the observed objects [15].

METHODOLOGY

Many of the techniques developed to enhance cloud-associated shadows ignore the information in the shadow regions. This is very clear when visually inspecting shadow areas, where energy indirectly reaching these areas is reflected to the sensor causing some details to appear in the image. Figure 1 presents parts of a runway and road intersection that are partially shown in shadow areas.

In our developed algorithm, the defected cloudy image is fused with another cloud-free image to form a new enhanced image from the high frequency components of the cloudy image and the low frequency information of the cloud-free image. Details shown in shadow areas due to energy indirectly reaching these areas were conserved. Figures 2 presents schematic diagrams of the methodology adopted in this approach. It should be mentioned here that the developed methodology of capturing and preserving high frequency component was applied in shadow areas only. Areas identified as clouds were simply replaced by corresponding areas in the cloud-free image.

Cloud/shadow Detection Algorithm: Cloud/shadow detection is the first step towards producing an enhanced

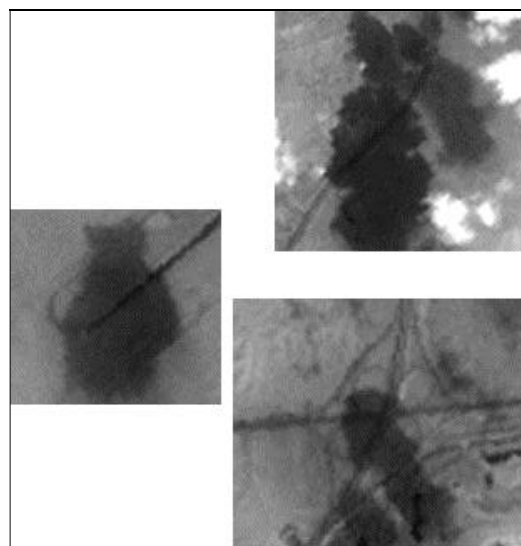


Fig. 1: Features partially obscured by cloud shadows

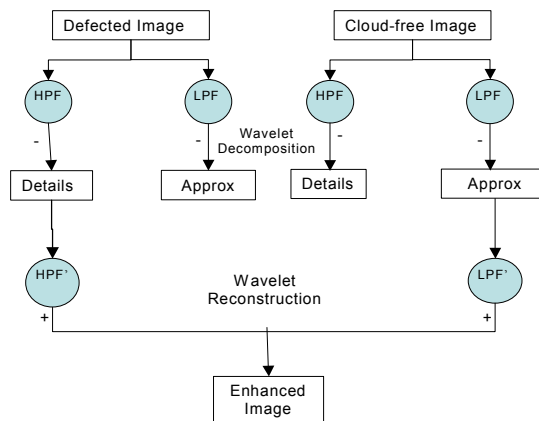


Fig. 2: Schematic representation of developed methodology

image. A technique developed by [9] that utilizes not only the spectral properties of the clouds and shadows, but also incorporates the spatial relationships between them is suggested. In this technique, the results of a neural network classification process, which mainly depends on performing automatic classification based on image spectral properties, are improved by defining the spatial relationship between cloud patches and their corresponding shadow patches.

A mathematical model for the spatial relationship is proposed and a least squares adjustment process is performed to estimate model parameters. Low spectral threshold is used to define shadow pixels resulting on more pixels mistakenly identified as shadow. The model is then used to filter out non-shadow pixels.

Image Fusion Using Discrete Wavelet Transform: The developed methodology suggests that both defected and cloud-free images are composed using discrete wavelet transform to create different high and low frequency components. The high frequency component contains image details such as noise, edges and details. On the other hand, the low frequency (approximation) components contain basic image information. Considering wavelet decomposition of the shadow areas of an image, it could be easily shown that the details components contain image information located in these areas.

Information beneath shadows could be preserved if the details information in these areas were used in the image reconstruction process while neglecting the approximation component. However, neglecting the approximation component produces an image with only high frequency information. To solve this problem, the approximation component of another cloud-free image was suggested to replace the approximation component of the defective image dominated primarily by the cloud-associated shadows. The developed wavelet-based image fusion technique is represented schematically in figure 2.

EXPERIMENTS AND RESULTS

Test Data: The developed technique is implemented on the panchromatic band of a November 2001 Landsat 7 ETM satellite subscenes, shown in Figure 3. Features in these images are partially obscured by cloud-associated shadows. For simplicity, boundary problems were solved by allowing the application to process the original scene outside the boundaries of the test subscenes when this is needed to perform the analysis.

Two cloud-free images, shown in Figure 4,5, were tested to enhance shadow areas in the defected cloudy image using wavelet fusion technique. The first cloud-free image is another ETM Panchromatic image of the same resolution taken in July 2000. The second test image is a 30 meters resolution Landsat ETM taken in May 2001. This image was pre-processed by conversion to gray level image and resampling to 15 meter pixel size.

Shadow Detection: The cloud/shadow detection algorithm described in section 3.1 was implemented on the cloudy image. This algorithm utilized image spectral characteristics and cloud/shadow spatial constraints for the detection. The results of the cloud and shadow identification step were two binary masks, one for clouds and the other for shadow regions. Figures 6 and 7 show the binary image of detected clouds and shadows for the study areas. Using manual digitizing as reference,



Fig. 3: Study area-Nov 2001 Landsat 7 ETM panchromatic sub-scene



Fig. 4: First cloud-free images-July 2000 Landsat7 ETM panchromatic subscene

computed values for the shadow classification results commission and omission errors were 11% and 9%, respectively.

Shadow Enhancement Using Discrete Wavelet Analysis: Two cloud-free images were used to implement the shadow removal technique using image fusion approach. The first cloud-free image is another ETM Panchromatic image of the same resolution. The second image is a 30 (resampled to 15) meter resolution Landsat ETM image composed of the three visible bands and converted to gray level image using band averaging algorithm. These two images were shown in Figures 4 and 5 above.



Fig. 5: Second cloud-free image–May 2000 Landsat ETM visible bands subscene converted to gray level image

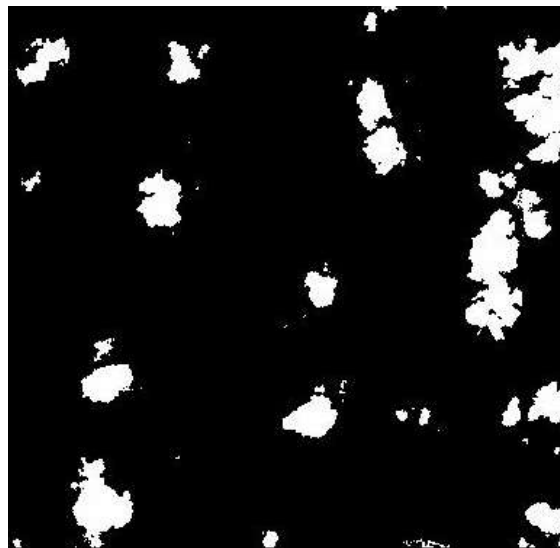


Fig. 7: Binary image for detected shadows in the study area

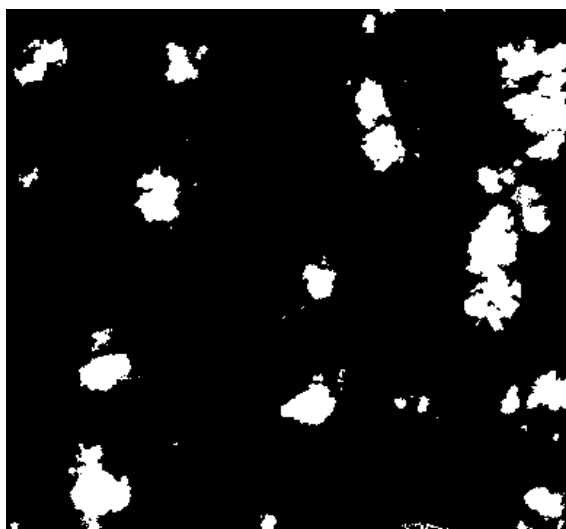


Fig. 6: Binary image for detected clouds in the study area

The defected image was composed using Bior 2,2 wavelet transform filter using Matlab Software. Figure 8 shows the decomposed images up to three decomposition levels. In this figure, we can notice that cloud areas do not show much high frequency content in the detail components. However, shadow areas contain high frequency components that represent underneath features (or noise).

The defected and the cloud-free images were decomposed to the same level of wavelet decomposition. The resulting image is then reconstructed from the high

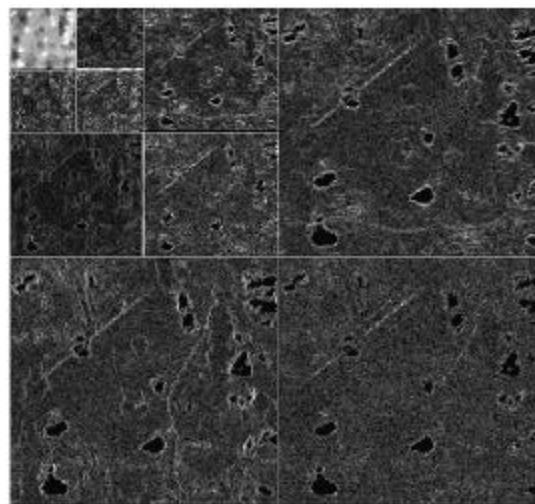


Fig. 8: Third level 'Bior 2,2' wavelet decomposition of defected image

frequency component of the wavelet decomposition of the original image and the low frequency component of the wavelet decomposition of the cloud-free image as presented in Figure 2. This approach could be looked at as a typical image fusion application based on wavelet decomposition utilized to filter out certain components in one of the images involved.

Testing several decomposition levels showed that details from the original image in the shadow area mostly exist in the detail components of the third wavelet decomposition level. However, image reconstruction of high and low frequency components of two different

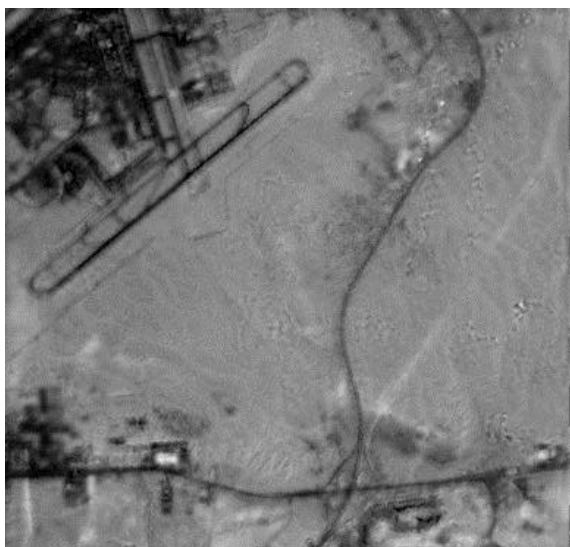


Fig. 9: Image reconstructed from second level decomposition of the cloudy image and the high-resolution cloud-free image

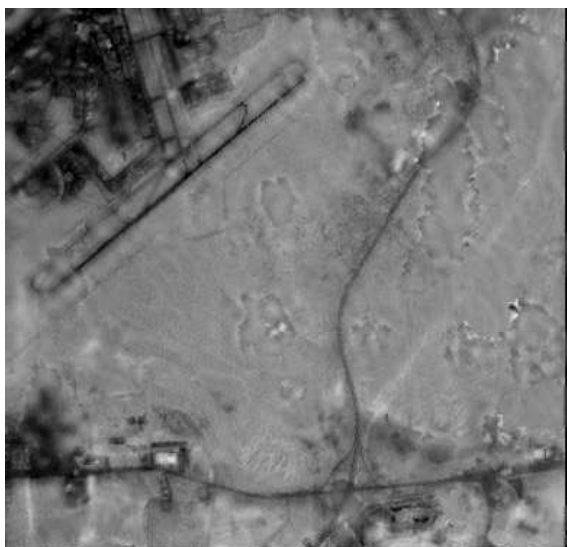


Fig. 10: Image reconstructed from third level decomposition of the cloudy image and the high-resolution cloud-free image

images results in many introduced artifacts in the produced image. These artifacts are due to differences in frequency content at each decomposition level of the participating images in addition to uncertainties in the space-frequency localization. Figures 9 and 10 show the resulting image after applying this approach using second and third wavelet decomposition levels.



Fig. 11: Cloud-free image with artificially masked details

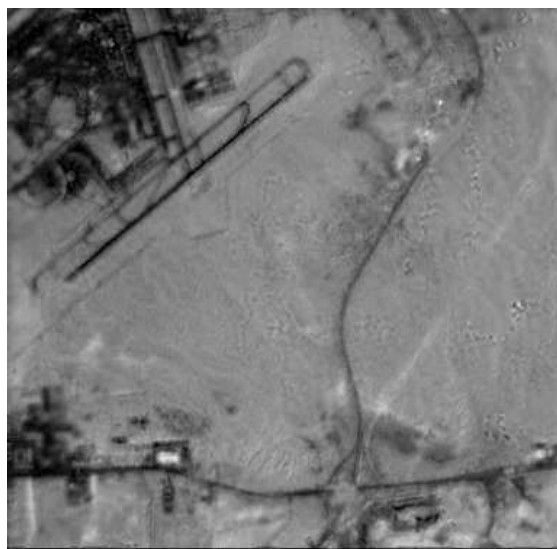


Fig. 12: Image reconstructed from second level decomposition of the cloudy image and the artificially altered high-resolution cloud-free image

Testing Details Capturing in Shadow Areas: To prove the concept of capturing details information in the shadow areas in the reconstructed image, the cloud-free image was artificially altered, as shown in Figure 11, by masking out details in areas where shadows exist in the defected image. These details should be obtained after applying the fusion process only from the shadow areas in the cloudy image.

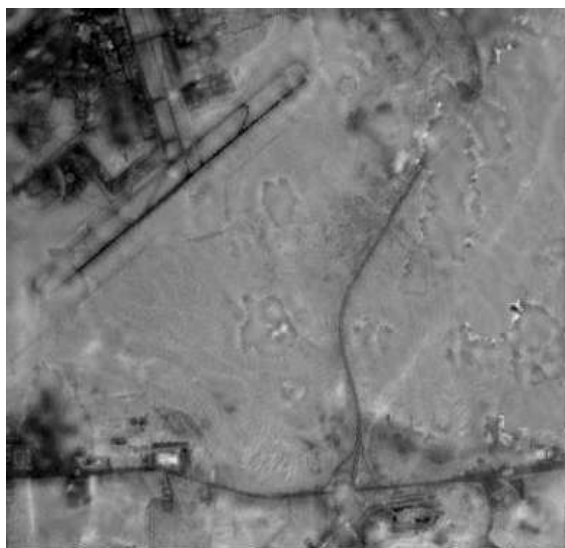


Fig. 13: Image reconstructed from third level decomposition of the cloudy image and the artificially altered high-resolution cloud-free image



Fig. 14: Image reconstructed from second level decomposition of the cloudy image and the low-resolution (resampled) cloud-free image

Figure 12 shows the image resulting from applying the fusion process using second level wavelet decomposition. In this figure, the details underneath shadows in the defected image were picked up in the resulting image although these details were masked out in the cloud-free image. Figure 13 shows the results of applying the same experiment using third level wavelet

decomposition. This figure shows that more details were picked from shadow areas in the cloudy image. However, the third level decomposition caused patchy image appearance and unwanted artifacts.

Fusion with Lower Resolution Imagery: The final test was performed by applying the technique using lower resolution cloud-free image. As described in section 4.1, the image is a 30 meter resolution Landsat ETM image resampled to 15 meters ground pixel size. A second level wavelet transform was used for the image fusion. The shadow enhancement result from this experiment is shown in Figure 14. Comparing the images in Figure 14 and 9, it could be noticed that more undesirable artifacts are shown in figure 14, which could be attributed to the differences in frequency content and distribution in the fused images. Moreover, the lower quality appearance of the image shown in figure 14 reflects the effect of using the approximation component of a lower resolution image in the fusion process.

CONCLUSION

A new technique for cloud-associated shadows elimination was developed. The technique was based on wavelet image decomposition and fusion with another cloud-free image. The developed technique was successful in enhancing cloud-associated shadow areas in the image while preserving details in the shadow areas. The ability to maintain these details increased with the increase of wavelet decomposition level. However, the higher this level is, the more artifacts in the output image. Generally, two or three wavelet decomposition levels were found to be sufficient for the analysis used in this study.

The results obtained using two images with the same spatial resolution were found to be better than those obtained when using images with different spatial resolution. This could be attributed to the differences in frequency content in the two fused images. More research is recommended in this area to determine the best decomposition components to participate in the fusing process according to each image's frequency content.

REFERENCES

1. Belward, A.S. and C.R. Valenzuela, 1991. Remote Sensing and Geographic Information Systems for Resource Management in Developing Countries, Kluwer Academic Publishers, London.

2. Finlayson, G.D., S.D. Hordley and M.S. Drew, 2002. Removing Shadows from Images, In Proc. of European Conf. on Computer Vision, 4: 823-836.
3. Marini, D. and A. Rizzi, 2000. A computational approach to color adaptation effects, *Image and Vision Computing*, 18(13): 1005-1014.
4. Zhou, G., Z. Qin, S. Benjamin and W. Schickler, 2003. Technical Problems of Deploying National Urban Large-scale True Orthoimage Generation. The 2nd Digital Government Conference, Boston, May 18-21, 2003, pp: 383-3871.
5. Berbar, M.A. and S.F. Gaber, 2004. Clouds and shadows detection and removing from remote sensing images, *Electrical, Electronic and Computer Engineering, ICEEC'04*, 2004 International Conference, 5-7 Sept. 2004, pp: 75-79.
6. Wang, B. and A. Ono, 1999. Automated Detection and Removal of Clouds and Their Shadows from Landsat TM Images. *IECE Transactions Inf.& Syst.*, (E82-D)2:453-460.
7. Prati, A., I. Mikic, R. Cucchiara and M.M. Trivedi, 2001. Comparative Evaluation of Moving Shadow Detection Algorithms, *IEEE CVPR Workshop on Empirical Evaluation Methods in Computer Vision*, Kauai, Hawaii, 9-14 December, 2001.
8. Lisens, G., P. Kempencers, F. Fierens and J. Van Rensbergen, 2000. Development of cloud, snow and shadow masking algorithms for Vegetation imagery, *Proceedings of Geoscience and Remote Sensing Symposium IGARSS 2000*, Honolulu, Hawaii, 24-28 July, 2000, 2: 834-836.
9. Shaker, I., A. Abd-Elrahman, A. Abdel-Gawad and M.A. Abdelwahab, 2005. Toward Removing Cloud and Shadow Effects in Satellite Images Using Image Fusion Techniques. *The Scientific Engineering Bulletin*, Faculty of Engineering, Ain Shams University, Cairo, Egypt, 40(2): 112-117.
10. Burrus, C.S., R.A. Gopinath and H. Guo, 1998. Introduction to Wavelets and Wavelet Transforms, a primer, Upper Saddle River, Prentice Hall, NJ.
11. Gens, R., V. Zoltan and C. Pohl, 1998. Image and data fusion concept and implementation of a multimedia tutorial, In: *Fusion of earth data*, Sophia Antipolis, France, 28-30 January, 1998, pp: 217-222.
12. Pohl, C., 1999. Tools and Method for Fusion of Different Spatial Resolution, *International Archives of Photogrammetry and Remote Sensing*, Valladolid, Spain, 3-4 June, 1999, 32, Part 7-4-3 W6.
13. Della, M.R.R., M. Fiani, A. Fortunato and P. Pistillo, 2004. Using the Data Fusion Technique for Producing Thematic Map, *The International Archives of the Photogrammetry, Remote Sensing and Spatial Information Sciences*, Vol. 34, Part XXX, pp: 721-726.
14. Brisco, B. and B. Brown, 1995. Multidate SAR/TM Synergism for Crop Classification in Western Canada, *Photogrammetric Engineering and Remote Sensing*, 61(8): 1009-1014.
15. Burt, P.J. and R.J. Kolczynski, 1993. Enhanced image capture through fusion. In: *Proc. Fourth International Conference on Computer Vision*, Berlin, Germany, pp: 173-182.